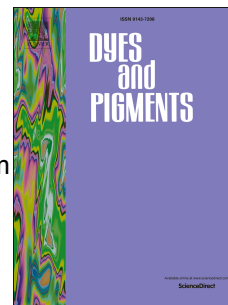


Journal Pre-proof

Remarkable mechanofluorochromism and low efficiency-off electroluminescence from a fully aromatic D-A cruciform emitter

Xin Xu, Lei Xu, Qikun Sun, Lingtai Yue, Yaguang Wang, Guangshui Yu, Haichang Zhang, Shanfeng Xue, Wenjun Yang



PII: S0143-7208(19)32814-1

DOI: <https://doi.org/10.1016/j.dyepig.2019.108170>

Reference: DYPI 108170

To appear in: *Dyes and Pigments*

Received Date: 2 December 2019

Revised Date: 18 December 2019

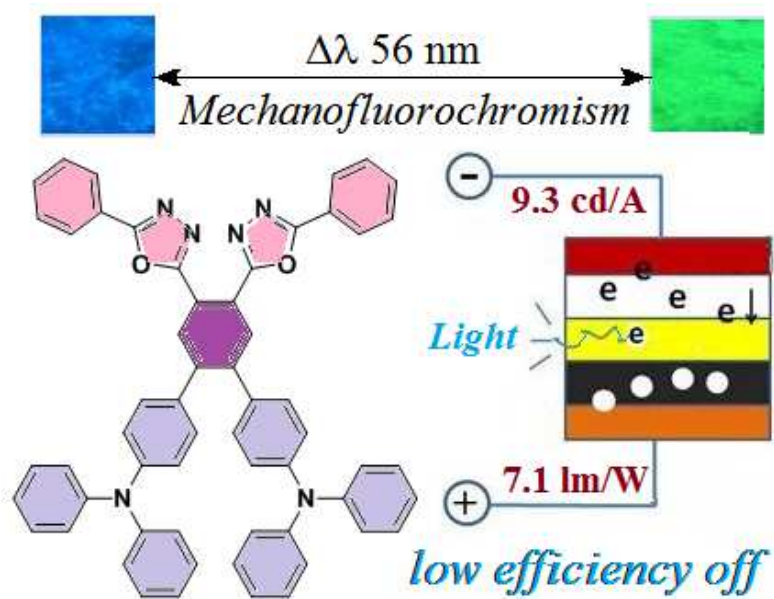
Accepted Date: 23 December 2019

Please cite this article as: Xu X, Xu L, Sun Q, Yue L, Wang Y, Yu G, Zhang H, Xue S, Yang W, Remarkable mechanofluorochromism and low efficiency-off electroluminescence from a fully aromatic D-A cruciform emitter, *Dyes and Pigments* (2020), doi: <https://doi.org/10.1016/j.dyepig.2019.108170>.

This is a PDF file of an article that has undergone enhancements after acceptance, such as the addition of a cover page and metadata, and formatting for readability, but it is not yet the definitive version of record. This version will undergo additional copyediting, typesetting and review before it is published in its final form, but we are providing this version to give early visibility of the article. Please note that, during the production process, errors may be discovered which could affect the content, and all legal disclaimers that apply to the journal pertain.

© 2019 Published by Elsevier Ltd.

Graphical Abstract



**Remarkable mechanofluorochromism and low efficiency-off electroluminescence
from a fully aromatic D-A cruciform emitter**

Xin Xu,[†] Lei Xu,[†] Qikun Sun, Lingtai Yue, Yaguang Wang, Guangshui Yu, Haichang Zhang, Shanfeng Xue,* Wenjun Yang*

Key Laboratory of Rubber-Plastics of Ministry of Education/Shandong Province (QUST),

School of Polymer Science & Engineering, Qingdao University of Science & Technology, 53-Zhengzhou Road, Qingdao 266042, P. R. China.

Xin Xu[†] and Lei Xu[†] contributed equally.

* Corresponding author: Shanfeng Xue, Email: sfxue@qust.edu.cn

* Corresponding author: Wenjun Yang, Email: ywjph2004@qust.edu.cn

Abstract:

Two-dimensional aryl center-crossed cruciforms generally exhibit the strongly twisted conformation and the spatial separation of frontier molecular orbitals, which can render the emitters destructible packing structures and high solid-state fluorescence efficiency. In the current work, we design and synthesize a benzene-centered cruciform emitter (DOT) with two adjacent phenyloxadiazoles and two adjacent triphenylamines starting from commercially available chemicals. Single crystal analysis indicates that DOT molecules loosely pack together in a twisted conformation and weak inter-molecular interactions. Upon mechanical grinding, the crystalline DOT is changed into an amorphous state, accompanying with a remarkable (56 nm) mechanofluorochromism (MFC). In view of the crossed donor and acceptor structure and the strong solid-state fluorescence, the non-doped electroluminescence (EL) devices with the structures ITO/HATCN/NPB or TAPC/DOT/TPBi/LiF/Al are

fabricated. The devices efficiently emit 500 nm green EL with the low turn on voltage of 2.7 V and the low efficiency roll-off. Thus, we have provided a feasible synthetic strategy for various isomers and analogues of fully aromatic benzene-centered D–A cruciforms and demonstrated a new class of candidates for MFC and EL materials.

Keywords: benzene-center cruciform; two-dimensional conjugated dye; electroluminescence; mechanofluorochromism; efficiency off

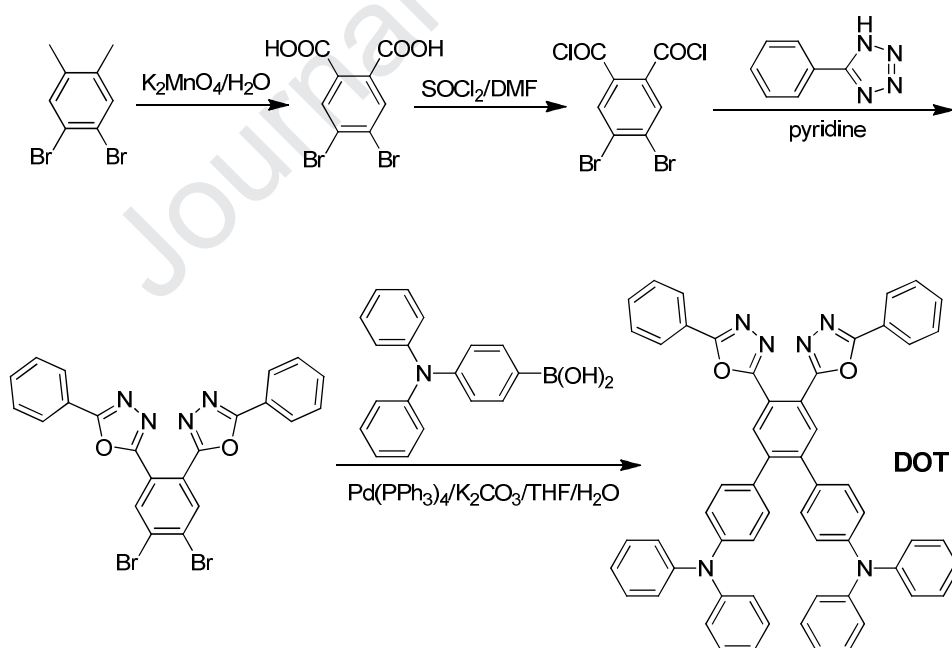
1. Introduction

Organic light-emitting materials are attracting much attention owing to their promising applications in light-emitting diodes, optical recording and anti-counterfeiting, etc.[1–11] Many conjugated organic molecules with diverse conformations and configurations have been designed and synthesized for obtaining multifunctional materials and improving optoelectronic properties. Among them, linear or one-dimensional conjugated organic molecules are ever the mainstay of advanced materials for optical and optoelectronic applications. In contrast, high dimensional organic molecules including conjugated organic framework and arylene-centered branched oligomers have started to draw research interest in recent years, which has expedited the appearance of some benzene-, anthracene-, benzobisoxazole-, pyrazine-centered cruciforms.[3, 12–15] These new configuration molecules have greatly widened the scope of material candidates in chemosensors, molecular switches, nonlinear optics,

field effect transistors, and photovoltaic and electroluminescence devices. While we have synthesized and investigated the asymmetrical π -center 2,6,9,10-tetra(arylvinyl)anthracene derivatives showing unique aggregation-enhanced one- and two-photon absorption and emission behaviors, we are now interested in symmetrical π -center benzene-cored cruciforms with fully aromatic donor and acceptor branches. It should be noted that the benzene-centered cruciforms with unsaturated double and triple bonds as conjugation bridge to link electron donors and acceptors have been synthesized and investigated widely,[16–20] including those with pyridine and dibutylamine as the end groups and sensing some positive ions.[21–27]

However, the fully aromatic benzene-centered conjugated cruciforms are rarely synthesized and investigated, to the best of our knowledge. Recently, Xu et al. synthesized a series of benzene-centered derivatives with two carbazoles and two diphenylphosphine oxide as the branches to serve as the blue thermally activated delayed fluorescence-emitting host to demonstrate the superiority of blue TADF-emitting host for high-efficient white light-emitting diodes.[28–32] Intrinsically, these molecules are not the real benzene-centered conjugated cruciforms due to the sp^3 -hybrid P atom. Samuel and Zysman-Colman et al. reported that the benzene-centered cruciforms with oxadizole and carbazole as branches are the thermally activated delayed fluorescence emitters.[33, 34] The doped organic light-emitting diodes can show the efficient blue electroluminescence but the high turn-on voltages of 3.85–4.60 V and the sharp

efficiency roll-off. We consider that conjugation length, molecular configuration, and donor and acceptor nature can seriously influence molecular conformation, intramolecular charge transfer, and aggregation state structure to tune the optoelectronic properties. Thus, a benzene-centered cruciform emitter with two adjacent phenyloxadiazoles and two adjacent triphenylamines as the branches, namely DOT (Scheme 1), is designed and readily synthesized. The results show that crystalline DOT can be ground into an amorphous state, accompanying with a remarkable (56 nm) mechanofluorochromism, and the non-doped light-emitting diodes with DOT as emitting layer efficiently emit green electroluminescence with the low turn on voltage of 2.7 V and the low efficiency roll-off.



Scheme 1. The structure and synthetic route for the fully aromatic benzene-centered cruciform DOT.

2. Experimental section

2.1 Materials

All solvents and reagents were of analytical grade and commercially available and used as received without further purification, unless otherwise claimed. 1,2-Dibromo-4,5-dimethylbenzene, 5-phenyl-1H-tetrazole, and (4-(di-phenylamino)phenyl)boronic acid were from Energy Chem. Co. Ltd., China.

2.2 Measurements

^1H and ^{13}C NMR spectra were recorded on a Bruker-AC500 (500 MHz) spectrometer with CDCl_3 as the solvent. Elemental analysis was performed on a Perkin-Elmer 2400. Photoluminescence spectra were recorded with a Hitachi F-4600 spectrophotometer, and the peak wavelength of the lowest energy absorption band was used as the excitation wavelength. Powder wide angle X-ray diffraction (PXRD) was performed on a Powder X-ray Diffractometer (INCA Energy, Oxford Instruments), operating at 3 kW. Differential scanning calorimetry (DSC) experiments were carried out on a Netzsch DSC 204F1 at a heating rate of $10\text{ }^\circ\text{C min}^{-1}$. Thermal gravimetric analysis (TGA) was undertaken on a Perkin-Elmer thermal analysis system at a heating rate of $10\text{ }^\circ\text{C min}^{-1}$ and a nitrogen flow rate of 80 mL min^{-1} . UV-vis absorption spectra were recorded on a Hitachi U-4100 spectrophotometer. Solution and solid-state fluorescence efficiency was determined with FLS980 Spectrometer equipping a integrating sphere. Mechanochromic luminescence and recovering experiments: a quantity of DOT solid was placed on a glass plate and simply ground by a metal spade. After the fluorescence color and spectrum was recorded, the

ground sample was put into an 180 °C oven and annealed for 5 min, and then kept for 1 min at room temperature before the measurements. The fuming experiment is to place the ground sample above the dichloromethane level and kept for 10 min at room temperature.

2.3 Device fabrication

Indium-tin oxide (ITO) coated glass with a sheet resistance of 15–20 Ω per square was used as the substrate. The substrate was prepatterned by photolithography to give an effective device size of 0.09 cm². It was then cleaned in an ultrasonic bath with acetone, detergent, deionized water, and isopropanol in a sequence, and dried in an oven. On the top of that, organic layers, dipyrazino[2,3-f.2',3'-h]quinoxaline-2,3,6,7,10,11-hexacarbonitrile (HATCN, 5 nm), *N,N'*-dinaphthyl-*N,N'*-diphenylbenzidine (NPB, 40 nm) or 1,1-bis[4-[*N,N'*-di(*p*-tolyl)amino]phenyl]cyclohexane (TAPC, 40 nm), emitting layer (DOT, 20 nm), and 1,3,5-tri(phenyl-2-benzimidazolyl)benzene (TPBi, 40 nm) were vacuum deposited in a sequence. Finally, a 1.0 nm thick LiF film and a 100 nm thick Al film were evaporated with a shadow mask to form the top electrode, at a base pressure of 3×10^{-4} Pa. The thickness of the evaporated cathodes was monitored using a quartz crystal thickness/ratio monitor (Model: STM-100/MF, Sycon). The effective luminous area of the device is 0.09 cm². Electroluminescence (EL) spectra were measured by a PR650 spectra scan spectrometer, and luminance–current density–voltage characteristics were recorded simultaneously with the measurement of the EL spectra by combining

the spectrometer with a Keithley model 2400 programmable voltage–current source. Measurements were carried out at room temperature ambient conditions.

2.4 Synthesis

4,5-Dibromophthalic acid.

In a 500 mL of two-neck flask, 1,2-dibromo-4,5-dimethylbenzene (10.2 g) and water (250 mL) were added. The mixture was heated to 100 °C and then KMnO_4 powder (24 g) was successively added in 10 portions within 2 h under stirring. After stirring for 8 h at 100 °C, the mixture was cooled to room temperature and sodium hydrogen sulfite (24 g) was added and stirred for 2 h. Further, KOH (16 g) was added and stirred for 2 h. The insoluble solid was filtrated and the filtrate was dropwise added sulfuric acid to precipitate the product. The white solid was collected and washed with water. The dried product (2.9 g, yield 24%) was used for next step without further characterization and purification.

5,5'-(4,5-Dibromo-1,2-phenylene)bis(2-phenyl-1,3,4-oxadi-azole).

4 mL of anhydrous DMF was added dropwise into a 100 mL of one-neck flask containing 4,5-dibromophthalic acid (2.6 g) and SOCl_2 (20 mL). After stirring for 8 h at 80 °C, the volatile liquids were removed by distillation. The residue (4,5-dibromophthaloyldichloride) in the flask was added pyridine (10 mL) and 5-phenyl-1H-tetrazole (2.6 g) and then stirred at 90 °C for 24 h. After removing the pyridine by rotating evaporation, ethanol was added to precipitate

the crude product. After separation by a column chromatography on silica gel using ethyl acetate/dichloromethane (1/10) as the eluent, the pure product was obtained (0.71 g, 24%). ¹H NMR (500 MHz): 8.40 (s, 2H), 7.93–7.89 (m, 4H), 7.51–7.46 (m, 2H), 7.40 ppm (dd, *J* = 8.5, 7.1 Hz, 4H). ¹³C NMR (125 MHz): 165.54, 161.48, 135.26, 132.13, 129.05, 126.92, 126.73, 123.27, 122.98 ppm. Anal. Calcd for C₂₂H₁₂Br₂N₄O₂: C, 50.41; H, 2.31; Br, 30.49; N, 10.69; O, 6.10. Found: C, 50.45; H, 2.33; N, 10.65%.

N⁴,N⁴,N^{4''},N^{4'''}-Tetraphenyl-4',5'-bis(5-phenyl-1,3,4-oxadiazol-2-yl)-[1,1':2',1''-terphenyl]-4,4''-diamine (DOT).

5,5'-(4,5-Dibromo-1,2-phenylene)-bis(2-phenyl-1,3,4-oxadiazole) (0.41 g, 0.78 mmol), (4-(diphenylamino)phenyl)boronic acid (0.54 g, 1.88 mmol), Pd(PPh₃)₄ (63 mg, 54 μmol), K₂CO₃ (0.16 g, 1.16 mmol), THF(20 mL), and H₂O (4 mL) were added into an 100 mL of flask and purged with nitrogen. The mixture was stirred for 48 h at 80 °C. The extracted organic phase with dichloromethane was dried over anhydrous magnesium sulphate and separated by a column chromatography on silica gel using ethyl acetate/dichloromethane (3/50) as the eluent. The separated product was further purified by re-crystallization from chloroform and vacuum sublimation. The yield is 85% (0.57 g). ¹H NMR (500 MHz): δ 8.20 (s, 2H), 7.94 (d, *J* = 7.7 Hz, 4H), 7.48 (t, *J* = 7.5 Hz, 2H), 7.40 (t, *J* = 7.7 Hz, 4H), 7.28 (d, *J* = 7.8 Hz, 8H), 7.13 (dd, *J* = 10.9, 8.6 Hz, 12H), 7.09–6.98 ppm (m, 8H). ¹³C NMR (125 MHz): δ 165.15, 163.34, 147.45, 147.35, 143.75, 132.67, 132.57, 131.81, 130.45, 129.32, 128.98, 126.85, 124.68,

123.38, 123.24, 122.51, 121.68 ppm. Anal. Calcd for $C_{58}H_{40}N_6O_2$: C, 81.67; H, 4.73; N, 9.85; O, 3.75. Found: C, 81.75; H, 4.70; N, 9.89%.

3. Results and discussion

3.1 Synthesis and solution photo-physical properties

The synthetic route and structure of DOT are depicted in the Scheme 1. Commercially available 1,2-dibromo-4,5-dimethylbenzene was oxidized to 4,5-dibromophthalic acid in an acceptable yield of 24%. This dried product was treated with dichlorosulfoxide, followed by reacting with 5-phenyltetrazole to afford 5,5'-(4,5-dibromo-1,2-phenylene)-bis(2-phenyl-1,3,4-oxadiazole). This is an useful intermediate because it can undergo the C-N coupling, the Heck coupling, and the Suzuki coupling to produce diverse conjugated cruciforms. When (4-(diphenylamino)phenyl)boronic acid was used to perform the Suzuki coupling, the target compound DOT was obtained in a high yield of 85%. The chemical composition and structure were confirmed by NMR spectra and elemental analysis. DOT is soluble in common organic solvents, and the solutions with the concentration of 10 μ M in hexane (Hex), triethylamine (TEA), butyl ether (BE), isopropyl ether (IPE), ethyl acetate (EA), tetrahydrofuran (THF), dichloromethane (DCM), acetonitrile (MeCN), and dimethyl formamide (DMF) are prepared. DOT solutions emit blue to orange fluorescence with peak emission wavelengths ranging from 453 to 575 nm upon increasing the solvent polarity (Figure 1), displaying a strong solvatochromic effect with a large spectral shift of 123 nm from hexane to DMF.

Figure 2 depicts the plot of the Stokes shift ($\nu_a - \nu_f$) versus the solvent polarity function f . The slope fitted according to the Lippert–Mataga equation affords a two-section curve. Although the two slopes are different, the continuing upward trends with the increase of solvent polarity are observed. Moreover, the quantum chemical calculations demonstrate that the HOMO electrons wholly localize on triphenylamine moieties and the LUMO electrons all concentrate on phenyl-oxadiazole branches (right side in Figure 2), a typical spatial separation of the frontier molecular orbital with few HOMO/LUMO overlap. These results indicate that DOT obviously shows the polarity-sensitive charge transfer (CT) state nature.

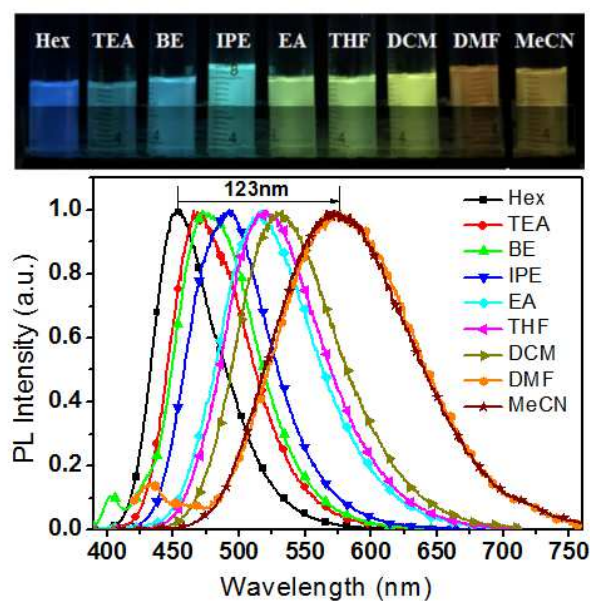


Figure 1. The fluorescence photos and emission spectra of DOT in different solvents under the excitation of 365 nm UV light.

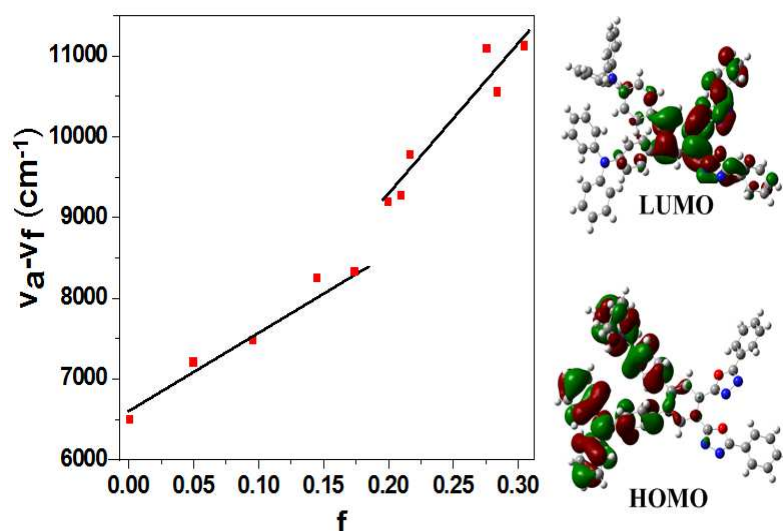


Figure 2. The plot of the Stokes shifts ($\nu_a - \nu_f$) versus the solvent polarity function (f) for DOT in various solvents and the calculated frontier molecular orbital nature.

3.2 Solid-state fluorescence and thermal properties

Organic luminophores can aggregate together in different stacking modes, depending on external stimuli (or preparation) conditions. Investigations on MFC materials and phenomenon have attracted much attention in the past decade.[35-37] However, the molecules with two-dimensional cruciform configuration are rarely exploited as MFC candidates. We investigate the MFC behavior of DOT solid under simple mechanical grinding on a glass plate using a metal spade. Powder X-ray diffraction patterns clearly indicate the grinding has induced a phase transformation from crystalline to amorphous states (Figure 3a). The diffraction pattern of the pristine DOT solid shows sharp and intense diffraction peaks, indicating a well-ordered microcrystalline structure. In contrast, the diffractogram of the ground DOT solid displays broad and

depressed reflections. As shown in Figure 4, the pristine solid emits blue fluorescence (462 nm) and can be readily changed into a green emission (518 nm) upon grinding, affording a remarkable color change and a large spectral shift of 56 nm. The grinding-induced amorphization is further evidenced by the differential scanning calorimetry (DSC) analysis (Figure 3b). DSC curves reveal that the pristine solid has no thermal transition before isotropic melting transition (257 °C), but the ground sample shows a glass transition temperature at 114 °C and a cold crystallization temperature at 150 °C. Notably, both pristine and ground solids exhibit the high fluorescence efficiency (47% and 56%, respectively). To examine MFC recovery, the ground sample is fumed on various volatile organic solvents and annealed between the glass transition and the cold crystallization temperatures (114–150 °C). It is found that the fluorescence color is only blue-shifted to blue-green and can not be recovered to the pristine blue color, signifying the not easy to crystallization of the amorphous state. We further anneal the ground sample above the cold crystallization temperature, such as at 170 °C, and find that the fluorescence color can be recovered to the pristine blue color. Regrinding the fumed and annealed samples can produce the same MFC effectiveness as the first grinding (Figure 4). Thus, the large and reversible MFC behavior happens only upon grinding and high-temperature annealing and is ascribed to the phase transition between crystalline and amorphous states.

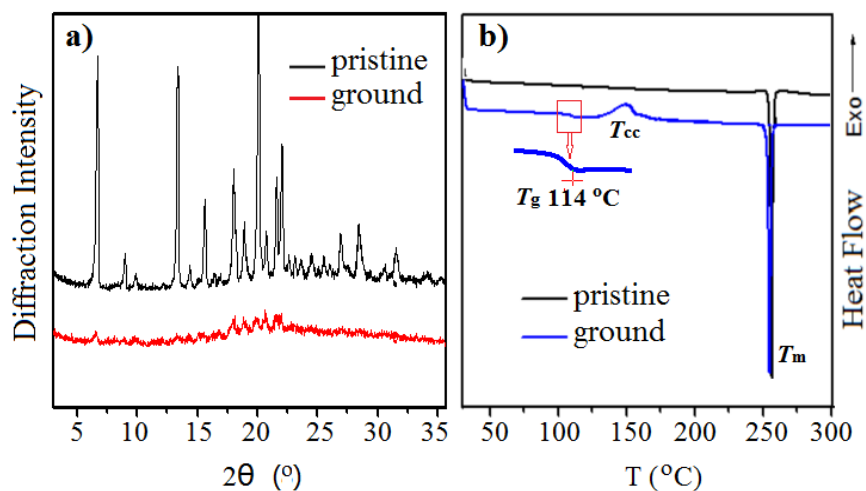


Figure 3. (a) X-ray diffraction curves and (b) DSC curves of DOT solids under pristine crystalline state and ground state.

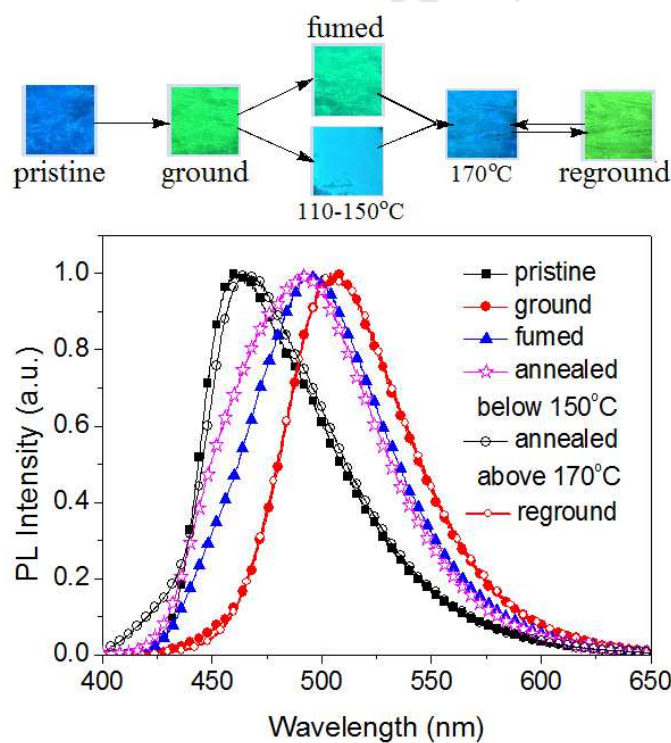


Figure 4. The fluorescence photos and emission spectra of DOT solids under different external stimuli.

Fortunately, we have obtained the analyzable single crystal of DOT (CCDC number: 1965820), which enable us to gain an insight into the

molecular packing mode to understand the high solid-state fluorescence efficiency and the destructible crystal structure. Single crystal analysis indicates the dihedral angles between the peripheral phenyl and oxadiazyl units are not large (8.58° and 18.4° , Figure 5) due to the weak intramolecular repulsion. However, the dihedral angles between the central benzene and oxadiazyl rings are large (33.9° and 37.7°) owing to the strong mutual repulsion of two adjacent oxadiazole rings. As expected, when two phenyls are ortho-linked to the same benzene ring, the very stronger mutual repulsion has resulted in the larger dihedral angles between the central benzene and the two connected phenyls (51.0° and 66.8°). Triphenylamine moieties are in the inherent propeller conformation. The two relatively strong interacted molecules are also shown in Figure 5, and 12 $\text{CH}\cdots\pi$ and 4 $\text{CH}\cdots\text{N}$ interactions are observed, which is not much and strong relatively for such a large-size molecule. Thus, DOT adopts a highly twisted conformation to loosely pack together with weak intermolecular interactions and without π - π interactions (Figure 5b), which should be favorable for the fluorescence emission and the disordering destruction of crystal structure under mechanical stimuli.

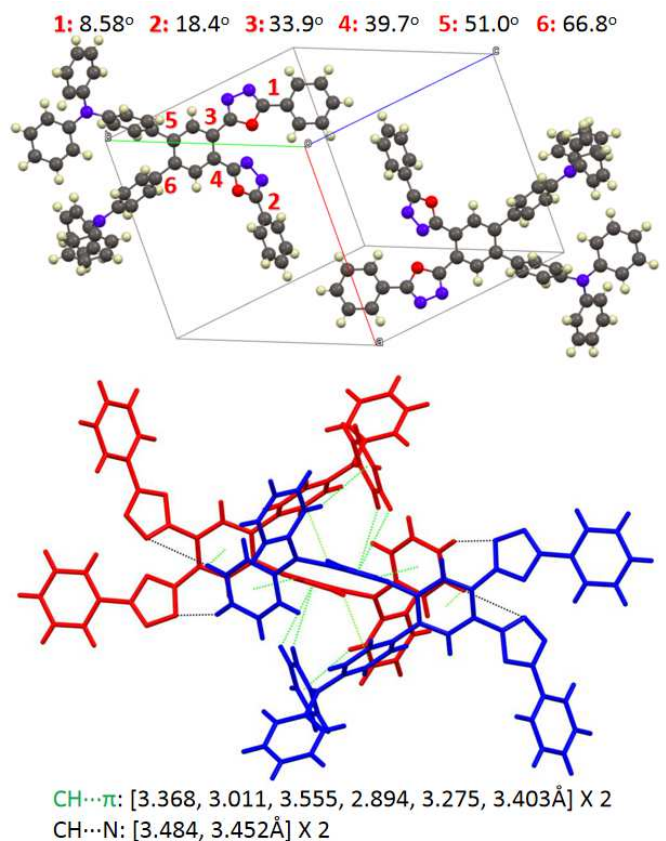


Figure 5. The cell structure, molecular dihedral angle, and the intermolecular interactions between two closely adjacent molecules in the single crystal.

3.3 Electroluminescence properties

Except for the admirable MFC and unique recovery behavior, DOT exhibits high fluorescence efficiency not only in solution and crystalline states but also in amorphous ground and film states. The fluorescence efficiency for the vacuum-evaporated film is up to 64.7%, which is even higher than the ground state (56%). In view of the high fluorescence efficiency and the donor- and acceptor-containing structure as well as the relatively high glass transition temperature (Figure 3b), DOT is expected to be a promising candidate as an efficient emitter for organic light-emitting diodes (OLED).

Devices with the structure ITO/HATCN (5 nm)/TAPC or NPB (40 nm)/DOT (20 nm)/TPBi (40 nm)/LiF (1 nm)/Al (100 nm) are fabricated, where HATCN, TAPC (device 1) or NPB (device 2), and TPBi are used as the hole-injection, hole-transport, and electron-transport/ hole blocking layers, respectively. Both device 1 and 2 exhibit same green-emitting electroluminescence (EL), and their EL spectra are also similar to the fluorescence spectrum of the vacuum-evaporated film (Figure 6).

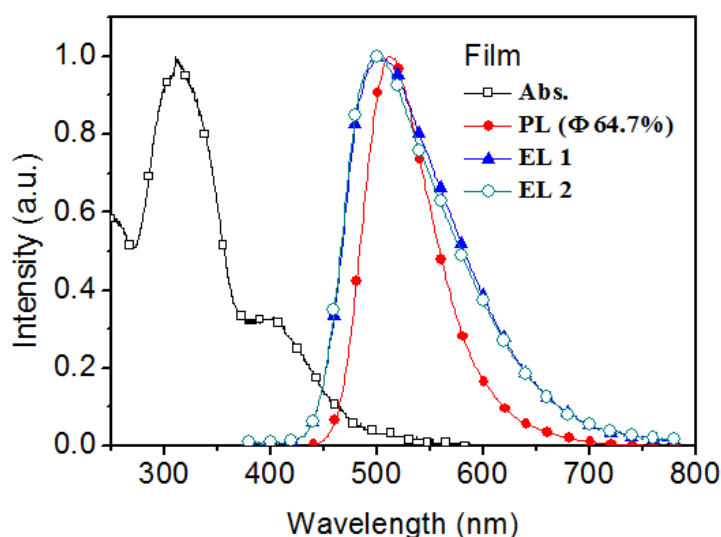
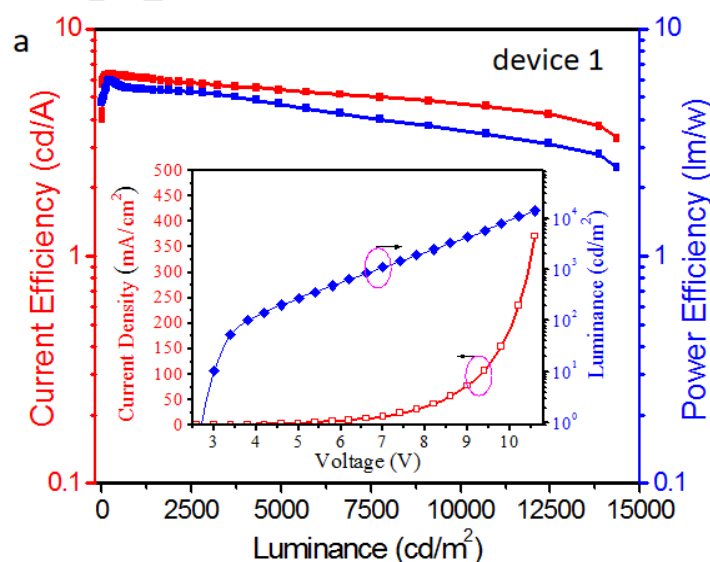


Figure 6. The absorption and photo-luminescence spectra of vacuum evaporated film and the electroluminescence spectra for the devices of ITO/HATCN/HTM/DOT/TPBi/LiF/Al, where the hole transport materials (HTM) are TAPC (device 1) and NPB (device 2), respectively.

The turn-on voltages of both devices are low at 2.69 V and 2.65 V, respectively. However, in spite of the same EL spectra and turn-on voltages, both devices exhibit very different EL performance (Figure 7). The maximum brightness is 14350 and 24500 cd/m^2 for devices 1 and device 2, respectively,

and the maximum current and power efficiency are 6.28 cd/A and 5.92 lm/W for device 1 and 9.27 cd/A and 7.05 lm/W for device 2. The low efficiency roll-off is also observed. For example, the current efficiency is 9.15, 9.21, 8.12 cd/A for the device 2 at the luminance of 100, 1000, and 10000 cd/m², respectively. These results indicate that DOT is an efficient emitter for fluorescence-based EL devices. It is noted that organic luminophors with strong twisted conjugation skeleton and loose intermolecular stacking are commonly unfavorable for carrier transporting. For that matter, the thinner emitter layer and the doped devices could boost the DOT potential to significantly improve EL performance. The device can exhibit better EL performance by employing NPB as the hole transport layer. Therefore, we predict that the device performance can be further improved by optimizing device compositions and structures, which is underway in our laboratory.



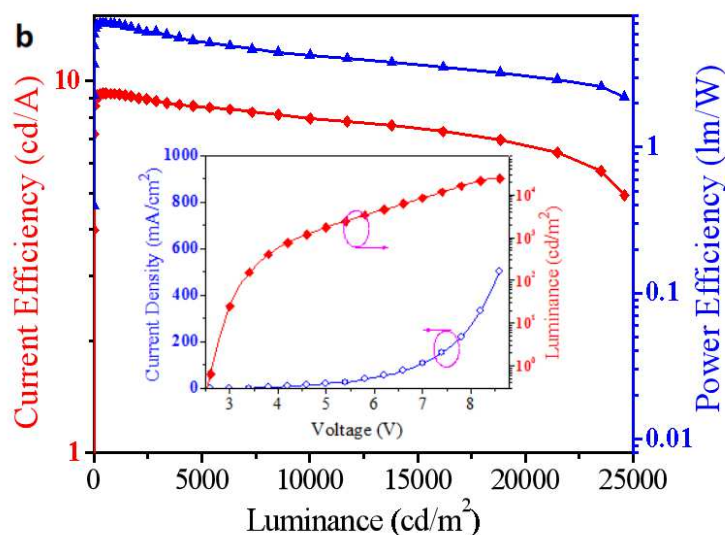


Figure 7. The current efficiency and power efficiency versus EL luminance curves for the device 1 (ITO/HATCN/TAPC/DOT/TPBi/LiF/Al) (a) and the device 2 (ITO/HATCN/NPB/DOT/TPBi/LiF/Al) (b). Inserts: The current density–voltage–brightness characteristics.

4. Conclusions

We have designed and synthesized a fully aromatic benzene-centered cruciform emitter (DOT) with two adjacent donors and two adjacent acceptors as the branches. The crowded substitution of four aryl branches on the same benzene ring has resulted in a strongly twisted conformation and loosely stacking structure, which render luminophores the destructible crystal structure and the high solid-state fluorescence efficiency. This kind of luminescent cruciforms could serve as promising mechanofluorochromism and light-emitting diode materials. We have demonstrated that DOT crystal can readily produce amorphization with a large spectral shift under simple mechanical grinding, and the non-doped devices exhibit the high luminance,

current efficiency, power efficiency, and the low turn-on voltage and efficiency roll-off. This work has also provided an effective synthetic strategy for a new class of fully aromatic benzene-centered cruciforms, and many isomers and analogues can be prepared by employing different xylenes and donors, which and the device optimization are underway in our laboratory.

5. Acknowledgements

Financial support for this research was provided by the National Natural Science Foundation of China (No. 51673105, 51873095 and 51573081), Natural Science Foundation of Shandong Province (No. ZR2018MB024), the Key Project of Higher Educational Science and Technology Program of Shandong Province of China (No. J18KZ001) and the Natural Science Foundation of Qingdao City of China (No. 16-5-1-89-jch). We thank the open project of The State Key Laboratory of Supramolecular Structure and Materials of Jilin University (SKLSSM-2019033).

6. Reference

- [1] Zhang T, Meng F, Lin L, Luo J, Wu H, Song X, et al. Theoretical study and experimental validation on the optical emission processes in "free" and "locked" pyrazine derivatives. *Spectrochimica acta Part A. Molecular and biomolecular spectroscopy*, 2019; 223: 117296.
- [2] Yang T, Liang B, Cheng Z, Li C, Lu G, Wang Y. Construction of Efficient Deep-Red/Near-Infrared Emitter Based on a Large pi-Conjugated Acceptor and

Delayed Fluorescence OLEDs with External Quantum Efficiency of over 20%.

Journal of Physical Chemistry C, 2019; 123(30): 18585-92.

[3] Park IS, Lee SY, Adachi C, Yasuda T. Full-Color Delayed Fluorescence Materials Based on Wedge-Shaped Phthalonitriles and Dicyanopyrazines: Systematic Design, Tunable Photophysical Properties, and OLED Performance. *Advanced Functional Materials*, 2016; 26(11): 1813-21.

[4] Zhang S, Yao L, Peng Q, Li W, Pan Y, Xiao R, et al. Achieving a Significantly Increased Efficiency in Nondoped Pure Blue Fluorescent OLED: A Quasi-Equivalent Hybridized Excited State. *Advanced Functional Materials*, 2015; 25(11): 1755-62.

[5] Bao C, Chen C, Muhammad M, Ma X, Wang Z, Liu Y, et al. Hybrid perovskite charge generation layer for highly efficient tandem organic light-emitting diodes. *Organic Electronics*, 2019; 73: 299-303.

[6] Triambulo RE, Kim J-H, Park J-W. Highly flexible organic light-emitting diodes on patterned Ag nanowire network transparent electrodes. *Organic Electronics*, 2019; 71: 220-6.

[7] Wang H-C, Bao Z, Tsai H-Y, Tang A-C, Liu R-S. Perovskite Quantum Dots and Their Application in Light-Emitting Diodes. *Small*. 2018; 14(1): 1702433.

[8] Kumar R, Sharma A, Singh H, Suating P, Kim HS, Sunwoo K, et al. Revisiting Fluorescent Calixarenes: From Molecular Sensors to Smart Materials. *Chemical Reviews*. 2019; 119(16): 9657-721.

[9] Singh E, Meyyappan M, Nalwa HS. Flexible Graphene-Based Wearable Gas and Chemical Sensors. *Acs Applied Materials & Interfaces*. 2017; 9(40): 34544-86.

- [10] Zhuang SQ, Shangguan RG, Huang H, Tu GL, Wang L, Zhu XJ. Synthesis, characterization, physical properties, and blue electroluminescent device applications of phenanthroimidazole derivatives containing anthracene or pyrene moiety. *Dyes and Pigments*. 2014; 101: 93-102.
- [11] Mukherjee S, Thilagar P. Organic white-light emitting materials. *Dyes and Pigments*. 2014; 110: 2-27.
- [12] Liao X, An K, Cheng J, Li Y, Meng X, Yang X, et al. High efficiency ultra-thin doping-free WOLED based on blue thermally activated delayed fluorescence inter-layer switch. *Applied Surface Science*. 2019; 487: 610-5.
- [13] Zhang H, Deng R, Wang J, Li X, Chen YM, Liu K, et al. Crystalline Organic Pigment-Based Field-Effect Transistors. *ACS Appl Mater Interfaces* 2017; 9: 21891–9.
- [14] Lim J, Albright TA, Martin BR, Miljanic OS. Benzobisoxazole Cruciforms: Heterocyclic Fluorophores with Spatially Separated Frontier Molecular Orbitals. *Journal of Organic Chemistry*. 2011; 76(24): 10207-19.
- [15] Zhang DT, Gao YY, Dong J, Sun QK, Liu W, Xue SF, et al. Two-photon absorption and piezofluorochromism of aggregation-enhanced emission 2,6-bis(p-dibutylaminostyryl)-9,10-bis(4-pyridylvinyl-2)anthracene. *Dyes and Pigments*. 2015; 113: 307-11.
- [16] Li J, Liu T, Zheng M, Sun M, Zhang D, Zhang H, et al. Dibutylaminophenyl- and/or Pyridinyl-Capped 2,6,9,10-Tetravinylanthracene Cruciforms: Synthesis and

Aggregation-Enhanced One- and Two-Photon Excited Fluorescence. *Journal of Physical Chemistry C*. 2013; 117(16): 8404-10.

[17] Lin J-A, Li S-W, Liu Z-Y, Chen D-G, Huang C-Y, Wei Y-C, et al. Bending-Type Electron Donor-Donor-Acceptor Triad: Dual Excited-State Charge-Transfer Coupled Structural Relaxation. *Chemistry of Materials*. 2019; 31(15): 5981-92.

[18] Tolosa J, Zuccherro AJ, Bunz UHF. Water-soluble cruciforms: Response to protons and selected metal ions. *Journal of the American Chemical Society*. 2008; 130(20): 6498-506.

[19] Xu DF, Hao JY, Gao HZ, Wang YH, Wang Y, Liu XL, et al. Twisted donor-acceptor cruciform fluorophores exhibiting strong solid emission, efficient aggregation-induced emission and high contrast mechanofluorochromism. *Dyes and Pigments*. 2018; 150: 293-300.

[20] Wang YH, Xu DF, Gao HZ, Wang Y, Liu XL, Han AX, et al. Mechanofluorochromic properties of aggregation-induced emission-active tetraphenylethene-containing cruciform luminophores. *Dyes and Pigments* 2018; 156: 291-8.

[21] Liu Y, Cui L-S, Xu M-F, Shi X-B, Zhou D-Y, Wang Z-K, et al. Highly efficient single-layer organic light-emitting devices based on a bipolar pyrazine/carbazole hybrid host material. *Journal of Materials Chemistry C*, 2014; 2(14): 2488-95.

- [22] Zhou G, Wong W-Y, Yang X. New Design Tactics in OLEDs Using Functionalized 2-Phenylpyridine-Type Cyclometalates of Iridium(III) and Platinum(II). *Chemistry-an Asian Journal*, 2011; 6(7): 1706-27.
- [23] Wild A, Winter A, Schluetter F, Schubert US. Advances in the field of pi-conjugated 2,2',6',2''-terpyridines. *Chemical Society Reviews*, 2011; 40(3): 1459-511.
- [24] Huang L-M, Tu G-M, Chi Y, Hung W-Y, Song Y-C, Tseng M-R, et al. Mechanoluminescent and efficient white OLEDs for Pt(II) phosphors bearing spatially encumbered pyridinyl pyrazolate chelates. *Journal of Materials Chemistry C*, 2013; 1(45): 7582-92.
- [25] Zuccherro AJ, McGrier PL, Bunz UHF. Cross-Conjugated Cruciform Fluorophores. *Accounts of Chemical Research*, 2010; 43(3): 397-408.
- [26] Mangalum A, Gilliard RJ, Jr., Hanley JM, Parker AM, Smith RC. Metal ion detection by luminescent 1,3-bis(dimethylaminomethyl) phenyl receptor-modified chromophores and cruciforms. *Organic & Biomolecular Chemistry*, 2010; 8(24): 5620-7.
- [27] Brombosz SM, Zuccherro AJ, Phillips RL, Vazquez D, Wilson A, Bunz UHF. Terpyridine-based Cruciform-Zn²⁺ complexes as anion-responsive fluorophores. *Organic Letters*, 2007; 9(22): 4519-22.
- [28] Xu S, Yang Q, Wan Y, Chen R, Wang S, Si Y, et al. Predicting intersystem crossing efficiencies of organic molecules for efficient thermally activated delayed fluorescence. *Journal of Materials Chemistry C*, 2019; 7(31): 9523-30.

- [29] Cho YJ, Yook KS, Lee JY. Cool and warm hybrid white organic light-emitting diode with blue delayed fluorescent emitter both as blue emitter and triplet host. *Scientific Reports*, 2015; 5: 7859.
- [30] Wex B, Kaafarani BR. Perspective on carbazole-based organic compounds as emitters and hosts in TADF applications. *Journal of Materials Chemistry C*, 2017; 5(34): 8622-53.
- [31] Cui Y, Jiang Y, Zhou L, Liu W, Zhu Q, Zhang H. High performance organic light-emitting diodes with tunable color range from orange to warm white based on single thermally activated delayed fluorescence emitter. *Optical Materials*, 2018; 85: 349-55.
- [32] Guo R, Hu D, Yue S, Zhang Z, Duan Y, Lu P, et al. Novel tetraarylsilan-centred compounds as single host for white organic light-emitting diodes with high efficiency and low roll-off. *Journal of Physics D-Applied Physics*, 2013; 46(26): 265101.
- [33] Giannini S, Carof A, Ellis M, Yang H, Ziogos OG, Ghosh S, et al. Quantum localization and delocalization of charge carriers in organic semiconducting crystals. *Nature Communications*, 2019; 10: 3843.
- [34] Wong MY, Zysman-Colman E. Purely organic thermally activated delayed fluorescence materials for organic light-emitting diodes. *Advanced Materials*, 2017; 29(22): 1605444.
- [35] Chi ZG, Zhang XQ, Xu BJ, Zhou X, Ma CP, Xu JR, et al. Recent advances in organic mechanofluorochromic materials. *Chemical Society Reviews*, 2012; 41: 3878-96.

[36] Zhao J, Zhang Y, Mao Z, Yang ZY, Chi ZG, et al. Recent progress in the mechanofluorochromism of cyanoethylene derivatives with aggregation-induced emission. *Journal of Materials Chemistry C*, 2018; 6: 6327-53.

[37] Di BH, Chen YL. Recent progress in organic mechanoluminescent materials. *Chinese Chemical Letters*, 2018; 29: 245-51.

Journal Pre-proof

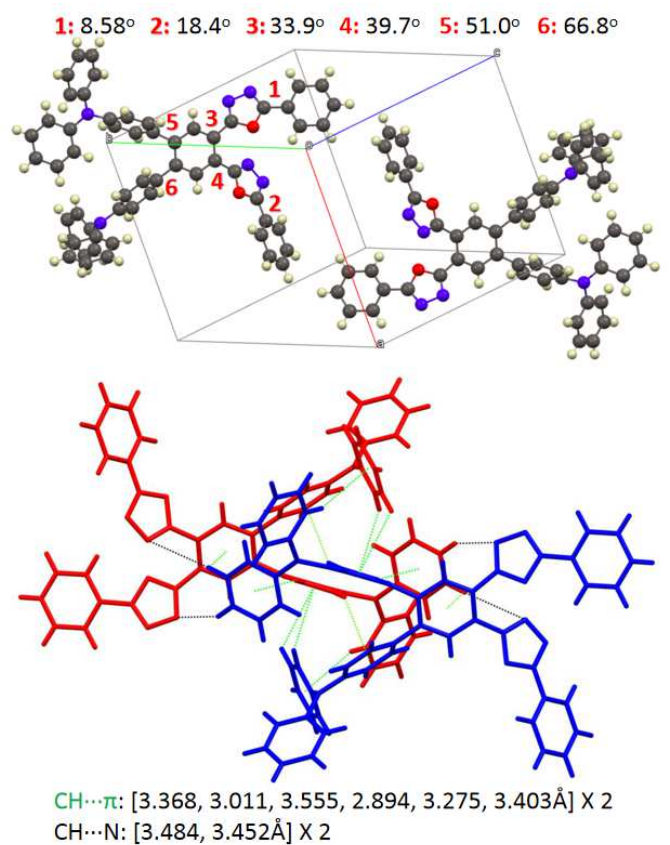


Figure 5. The cell structure, molecular dihedral angle, and the intermolecular interactions between two closely adjacent molecules in the single crystal.

Highlight:

1. A new two-dimensional conjugated molecule is designed and synthesized
2. Crossed donor-acceptor molecules show high light-emitting efficiency
3. Cruciforms with strong twisted structure are easy to mechanofluorochromism
4. A non-doped EL device with low efficiency off is achieved

Xin Xu and Lei Xu conducted the synthesis and the photophysical characterizations of the materials. Lei Xu and Lingtai Yue fabricated the OLED for the materials and estimated the OLED performances. Qikun Sun analyzed the single crystal structure. Yaguang Wang did the theoretical calculations. Guangshui Yu is responsible for the basic testing and analysis of thermal and electrochemical properties. Haichang Zhang tested and analyzed the mechanofluorochromism properties. Xin Xu and Lei Xu wrote the paper, and all the authors revised it. Shanfeng Xue and Wenjun Yang supervised the whole work. Xin Xu and Lei Xu contributed equally to this work.

Declaration of interests

The authors declare that they have no known competing financial interests or personal relationships that could have appeared to influence the work reported in this paper.

The authors declare the following financial interests/personal relationships which may be considered as potential competing interests:

Journal Pre-proof